



OPEN

Diffusion-induced lithium isotopic heterogeneity in olivines from peridotites of an oceanized mantle lithosphere at the Yunzhug ophiolite (central Tibet)

Ren-Deng Shi¹✉, Guang-hao Cui^{1,2}, Qi-Shuai Huang¹, Xiao-Xiao Huang³, Haibo Zou⁴, Xiaohan Gong⁵ & Jing-Sui Yang⁶

This paper reports lithium concentrations and isotopic compositions of olivines in the oceanized subcontinental lithospheric mantle (SCLM) peridotites of the Tibetan Yunzhug ophiolite. The results show systematic Li isotope changes with distance from the rim of olivine grains. $\delta^7\text{Li}$ values of olivine in dunites decrease from +10.46 to +1.33‰ with increasing distance to olivine rim from 26.15 to 124.71 μm . A negative correlation of $\delta^7\text{Li}$ and Li content in olivine from dunite and harzburgite indicates recent diffusive ingress of Li into the peridotites. The extremely heavy Li isotopic composition requires the seawater or seawater alteration endmember in the mixing model, and reveals Li diffusion from seawater into olivine. As in dunites, olivines in a harzburgite sample show similar variations in $\delta^7\text{Li}$ as a function of distance from the grain rim (e.g., 6.01 to 1.73 in sample 14YZ13). We suggest that the behavior of Li in the oceanized SCLM peridotites may be controlled by Li diffusion from seawater, as Li activity in the liquid state is higher than the solid state in transporting Li through the olivines in the peridotites. This study supports that seawater Li diffusion is one of the important factors for the heterogeneity of mantle Li isotopes in ophiolites.

Keywords Li isotopes, Heterogeneity, Seawater diffusion, SCLM peridotite, Tibetan Yunzhug ophiolite

High-temperature processes are generally considered as important factors of mantle isotope heterogeneity, such as the interaction of lithosphere and mantle plume and the recycling of oceanic lithosphere at different stages of Wilson cycles^{1–7}. High-temperature processes are often used to explain the isotopic heterogeneity of mantle peridotite in ophiolites. Such interpretations of isotopic heterogeneity in ophiolites are certainly suitable for lithophile and siderophile element tracers such as Sm–Nd, Lu–Hf, Re–Os and Mg–Fe high-temperature isotopic systems⁸, but are not necessarily suitable for fluid-mobile Li in ophiolites. Lithium isotopes are useful not only for tracing crust–mantle recycling in subduction system, but also for studying low temperature fluid–rock interactions, due to the high solubility of lithium in melts/fluids, the large relative mass difference between ⁷Li and ⁶Li, and the higher diffusivity of ⁶Li relative to ⁷Li^{9,10}. Li isotopes can be strongly fractionated at low temperatures with $\delta^7\text{Li}$ values of +31‰ in seawater¹¹. Thus, the surficial process also could change Li isotope composition of oceanic lithospheric rocks on the seafloor by seawater–rock exchange at low temperature. For example, seawater–basalt exchange could produce Li enrichment and a $\delta^7\text{Li}$ increase in altered basalts^{12,13}, and during serpentinization of oceanic peridotites, ‘relict’ olivine and pyroxenes generally have lower Li concentrations and higher $\delta^7\text{Li}$ values as a result of Li diffusion in seawater¹⁴. Thus, the near-surface geological process is an important factor in producing Li isotope heterogeneity in the mantle sequence of ophiolite.

¹State Key Laboratory of Tibetan Plateau Earth System, Environment and Resources (TPESER), Institute of Tibetan Plateau Research, Chinese Academy of Sciences, Beijing 100101, China. ²University of Chinese Academy of Sciences, Beijing 100049, China. ³College of Geosciences and Engineering, North China University of Water Resources and Electric Power, Zhengzhou 450045, China. ⁴Department of Geosciences, Auburn University, Auburn, AL 36849, USA. ⁵School of Ocean Sciences, China University of Geosciences, Beijing 100083, China. ⁶School of Earth Sciences and Engineering, Nanjing University, Nanjing 210023, China. ✉email: shirendeng@itpcas.ac.cn

Ophiolites are generally considered as pieces of suboceanic lithospheric mantle that have been thrust onto the edges of continental plates^{15,16}. Mantle peridotite is a diagnostic unit of ophiolites. The peridotite from the Yunzhug ophiolite (Tibet) is a product of oceanization of subcontinental lithospheric mantle during the incipient rifting of the Gondwana continent, tectonically exposed on the ocean floor by large-scale detachments¹⁷. We selected olivines from peridotites of this ophiolite for a detailed in-situ Li isotope study to understand the ophiolitic mantle heterogeneity at the early stage of the Wilson cycle.

Geological setting and sample descriptions

The Yunzhug ophiolite, located northeast of Xainxa county in central Tibet, is in the middle part of the Shiquanhe-Namco ophiolite belt which is the southern boundary of the Bangong-Nujiang suture zone (BNSZ). The BNSZ extends approximately 1200 km across central Tibetan Plateau and separates the Lhasa terrane to the south and the Qiangtang terrane to the north. The Yunzhug ophiolite is mainly composed of ophiolitic blocks and thick sequences of Jurassic flysch and associated volcanic rocks. The ophiolitic massifs are up to 200 km long in the middle sector of BNSZ referred to as the Northern Tibetan Neo-Tethyan ophiolites^{18–21} (Fig. 1).

Mantle peridotite as the main component of the Yunzhug ophiolite crops out about 200 km², accounting for more than 90% in volume of the ophiolite. Associated mafic lavas are minor. The isolated ophiolitic massifs oriented in a NWW-SEE direction, are surrounded by Paleozoic–Mesozoic strata, and contain many autoclastic and exotic blocks. Small amounts of radiolarian cherts associated with the lavas are between Late Triassic and Late Cretaceous in age. The predominant serpentinized harzburgites are crosscut by centimeter- to decimeter-scale pyroxenite and meter-scale banded and laminated dunite. Compared with the classical Penrose ophiolite sequence in the relative positions of the various lithologies, the Yunzhug ophiolite differs from the traditional Cyprus ophiolite²² and Oman ophiolite²³. However, it is comparable with the Alpine-Apenne ophiolites²⁴, and displays strong similarities with the lithospheric structure of the Iberia-Newfoundland margin characteristic of young passive continental margins¹⁷.

The mantle peridotites studied here are mainly harzburgites with minor dunites that were slightly serpentinized. Fresh minerals are preserved widely in most harzburgites and locally in some dunites. The fresh mineral grains are mainly olivines with Fo values ranging from 91.8 to 93.8. Orthopyroxene (Opx) is generally found as 3 to 5 mm porphyroclasts. Compositionally, the Opx is magnesian (Mg# = 91.7–93.3). Their Al₂O₃ (0.45–1.55 wt%) and CaO content (usually 0.5–1.0 wt%, and less than 1.40 wt%) are consistent with those Opx from on-craton garnet lherzolites. Clinopyroxene (Cpx) has lower Al₂O₃ and Na₂O, and elevated Cr₂O₃ contents with an embryonic oceanic-crust affinity. The low Os isotopic compositions (¹⁸⁷Os/¹⁸⁸Os = 0.11301–0.12374; T_{RD} = 2.30–0.54 Ga) and high Mg# values of whole rocks and high Fo in olivine indicate that the peridotites originated from ancient subcontinental lithospheric mantle (SCLM). The fine-grained mineral clusters reflect modification of the peridotite massif, representing the oceanization process during the incipient rifting of the Gondwana continent¹⁷.

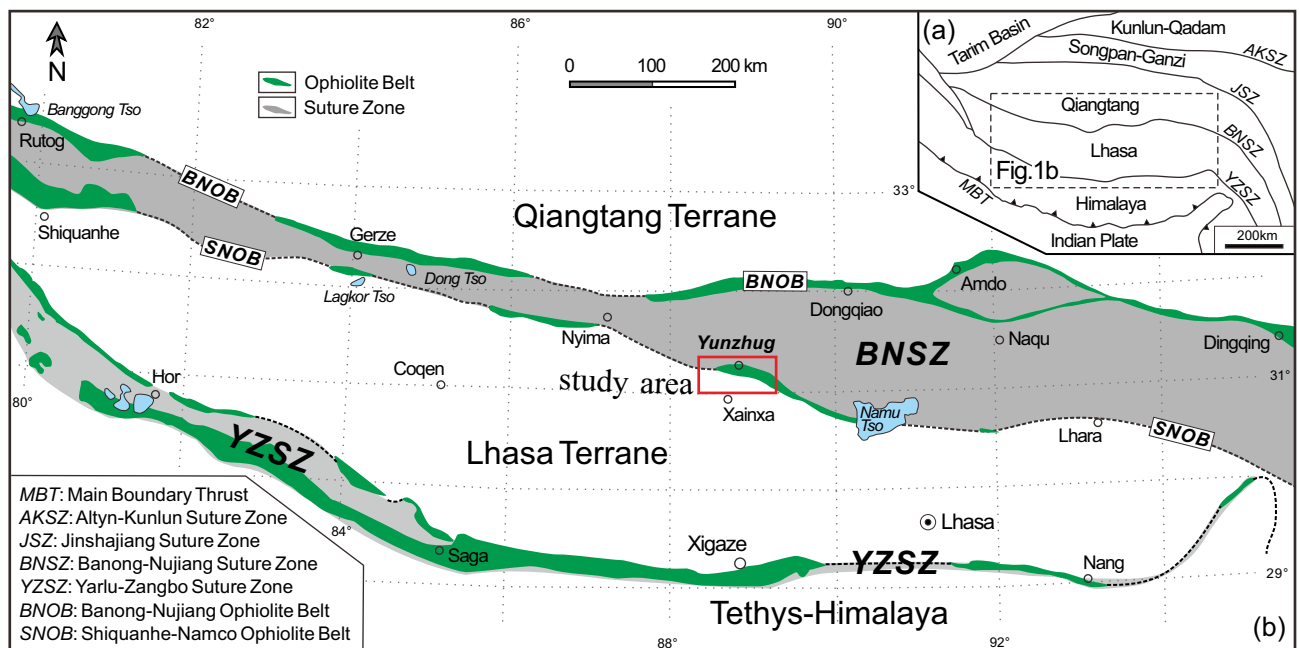


Figure 1. (a) Tectonic framework of Tibet and adjacent India, showing position of Bangong-Nujiang Suture Zone (BNSZ); (b) tectonic map of BNSZ showing the relationship between BNSZ and Bangong-Nujiang Ophiolite Belt (BNOB) and Shiquanhe-Namco Ophiolite Belt (SNOB) and other ophiolite belt (e.g. Naqu), and location of the Yunzhug ophiolite in Xainxa area¹⁶.

Lithium concentrations and isotopic compositions in olivines

Lithium concentrations and isotopic compositions ($\delta^7\text{Li}$) for both dunites and harzburgites are reported in Table 1 and plotted in Figs. 2 and 3a as a function of a distance from the rim of each olivine grain. The detailed information of $\delta^7\text{Li}$ and the distance from the rim (d) are shown in Fig. 3a. Lithium contents of the olivine grains analyzed here are different between dunite and harzburgites. Comparable to the estimate of the upper mantle Li content (2.00 ppm)^{25,26}, olivines in dunites have generally higher Li concentrations ranging from 2.13 to 3.55 ppm (with the exception of one grain at 1.80 ppm) than those in harzburgite (1.11–1.83 ppm). There are large variations in Li isotopic compositions of olivines. The correlation between Li isotopic composition and Li content of olivine in dunite is better than that in harzburgite. $\delta^7\text{Li}$ values of olivine plot along the mixing line between seawater and subcontinental lithospheric mantle (Fig. 3b).

Interestingly, the Li isotopic composition ($\delta^7\text{Li}$) is negatively correlated with the distance from the grain rim. $\delta^7\text{Li}$ values of olivines increase from 1.33 to 10.46‰ with a decreasing distance to the rim from 124.71 to 26.15 μm in dunites (Figs. 2, 3a). This negative correlation is supported by the data in individual olivine grains. In sample 14YZ-167, points 9, 10, 11 represent different distances in an individual olivine grain, and their Li isotopic compositions are negatively correlated with the distance to the rim. Point 9 has the highest $\delta^7\text{Li}$ value (3.17) with the shortest distance (60.3 μm), while point 11 has the lowest $\delta^7\text{Li}$ value (1.33) with the longest distance (124.7 μm), and the point 10 is intermediate in $\delta^7\text{Li}$ value and distance. The correlation between Li isotopic composition and the distance from the grain rim for harzburgites is not as good as that of dunites. Nevertheless, the rim of olivine grains from harzburgites still has higher $\delta^7\text{Li}$ value relative to the center of the grains.

Discussion

Ophiolitic mantle peridotites generally undergo at least three processes. The first stage is partial melting of convective upper mantle or primitive upper mantle to produce early harzburgites or dunites; the second stage is refertilization of the early harzburgites or dunites to form Cpx-free harzburgite and Cpx-bearing lherzolite via melt-rock interaction during seafloor spreading or subduction; and the third stage is serpentinization that has pervasively developed in the ophiolitic mantle sequence^{5,26–30}. The Yunzhug ophiolitic mantle peridotites are products of oceanization from ancient subcontinental lithospheric mantle (SCLM)¹⁷. Li abundance and isotopic composition of SCLM is useful for studying the oceanization processes of the ancient SCLM during the early stage of the Wilson cycle.

Homogeneous reservoirs in the mantle with $\delta^7\text{Li}$ around +4‰ have been estimated from the isotopic signatures of OIB and MORB²⁵. The studies of peridotite xenoliths hosted in volcanic rocks is another approach to estimate the Li isotopic composition of the upper mantle³¹. Lithium isotopic compositions in some mantle xenoliths and especially the clinopyroxene display a large range²⁸. Recent studies show a narrower range of $\delta^7\text{Li}$ in peridotite xenoliths from various tectonic settings^{32–34}, and most $\delta^7\text{Li}$ values are clustered around +2–4‰ within the range of the normal mantle value (Fig. 3b). Therefore, it is reasonable to use this value as mantle endmember for binary mixing calculation to reveal the characteristics of the samples. The result presented in Fig. 3a demonstrates correlations between Li concentrations and Li isotopic compositions of the olivines from the Yunzhug ophiolitic peridotites, which can be used to infer the possible geological processes and factors that control the Li isotopic composition of the oceanized SCLM.

Lithium diffusion in solid materials (e.g., Ol, Opx and Cpx) is much slower than in melt or fluids. The diffusion of Li into solid materials from an infinite source of Li, such as a surrounding fluid or melt, can be used to explain the Li isotopic disequilibrium of peridotites. Lithium elemental and isotopic disequilibrium of peridotites is produced by the recent melt/fluid-rock reaction or by the last stage serpentinization, as Li isotopes can be strongly fractionated at low temperatures. During the first stage of partial melting and the second stage of refertilization at high temperatures, Li isotopes should approach equilibrium. During the oceanization of ancient SCLM at the early stage of Wilson cycle, serpentinization is the last process of the formation of the ophiolitic mantle peridotites in the continental margin, where seawater circulates and interacts with peridotites. Lithium is a fluid-mobile element and its isotopes can be strongly fractionated at low temperature. Therefore, Li diffusion between seawater and fresh minerals (i.e., Ol) in peridotites is likely to determine the Li elemental and isotope characteristics of the oceanization SCLM. The marked Li isotopic disequilibrium in the olivines from Yunzhug ophiolitic peridotites is likely the product of such diffusion-driven kinetic isotopic fractionation. This scenario is similar to that of Li isotopic characteristics of minerals in the Zabargad peridotites (Fig. 3b) in the Red Sea³⁵, which is produced by the active rifting of continent (future ocean-continent-transition (OCT)-type ophiolite), but differs from the olivines in the abyssal peridotites³⁶ and the Trinity ophiolitic peridotites³⁷ that represent MOR- and SSZ-type ophiolites³⁸, respectively.

The negative relationship between the $\delta^7\text{Li}$ values and the distance from the analysis spot to the rim of the olivines indicates that the Li isotopes in olivines from the Yunzhug oceanization of the ancient SCLM (Fig. 3a) may be controlled by the seawater Li diffusion at the temperature conditions for serpentinization of shallow oceanic crust. As the rifting of ancient continent, the SCLM was gradually exposed to the surface and the hydrothermal convection of seawater permeates through newly formed, still hot oceanic crust and SCLM as shown in Fig. 4, which is supported by previous studies on metamorphism, mineralization and ferromanganese sediments³⁹. The thermal gradient in this single-pass system is greater than 150°C/km^{40,41}, and there is enough energy for Li to diffuse from seawater into fresh olivine during the early stage of Wilson cycle. Generally, this diffusion process may involve two steps. The first step occurs prior to serpentinization, where the Li diffusion-induced isotopic heterogeneity took place between the seawater and olivines. The second step occurs after serpentinization, where Li element in the serpentine with seawater Li isotopic features move to relics of olivines. During the first step, ^6Li and ^7Li move together into olivine grain by diffusion without obvious isotopic fractionation because of the small isotopic fractionation (the diffusivity ratio $D^7\text{Li}/D^6\text{Li}$ value is close to 1) in the seawater under the low-middle

Sample @ spot	Rock type	$\delta^7\text{Li}$	1SE	Li (ppm)	1SE	Distance from rim (μm)
14YZ-13OL@1	Harzburgite	1.83	0.90	1.83	0.010	50.4
14YZ-13OL@2		4.98	0.90	1.62	0.009	21.6
14YZ-13OL@3		4.15	0.89	1.63	0.008	40.8
14YZ-13OL@4		2.32	1.00	1.54	0.008	24.0
14YZ-13OL@5		1.73	0.98	1.57	0.008	26.4
14YZ-13OL@6		6.01	0.96	1.58	0.007	28.8
14YZ-13OL@7		3.84	0.98	1.49	0.007	28.8
14YZ-191OL@1	Harzburgite	4.51	0.96	1.17	0.005	76.9
14YZ-191OL@2		6.11	0.97	1.19	0.006	74.5
14YZ-191OL@3		4.22	0.97	1.45	0.007	72.1
14YZ-191OL@4		4.32	1.02	1.23	0.006	74.5
14YZ-191OL@5		4.51	1.02	1.12	0.006	69.7
14YZ-191OL@6		8.34	0.96	1.27	0.006	57.6
14YZ-191OL@7		3.90	1.20	1.11	0.005	74.5
14YZ-191OL@8		5.69	0.98	1.15	0.006	69.7
14YZ-163OL@1	Dunite	8.77	0.92	2.17	0.017	43.8
14YZ-163OL@2		7.25	0.91	2.73	0.019	64.6
14YZ-163OL@3		7.37	0.84	2.93	0.013	62.5
14YZ-163OL@5		8.43	0.91	2.77	0.018	45.8
14YZ-163OL@6		7.80	0.90	2.76	0.016	52.1
14YZ-163OL@7		7.79	0.85	2.54	0.024	51.9
14YZ-163OL@8		9.27	0.90	3.20	0.020	41.7
14YZ-163OL@9		8.86	0.86	2.15	0.012	43.8
14YZ-163OL@10		7.42	0.85	3.32	0.022	44.8
14YZ-163OL@11		8.35	0.85	3.10	0.020	41.7
14YZ-163OL@12		8.42	0.87	2.43	0.017	41.7
14YZ-163OL@13		6.31	0.84	2.90	0.018	62.5
14YZ-165OL@1		Dunite	3.69	0.83	3.81	0.025
14YZ-165OL@2	7.88		0.91	2.41	0.018	38.2
14YZ-165OL@4	10.46		0.91	1.80	0.010	26.1
14YZ-165OL@5	5.99		0.85	3.24	0.016	80.5
14YZ-165OL@6	7.39		0.92	2.79	0.013	62.4
14YZ-165OL@7	9.61		0.89	2.10	0.011	58.3
14YZ-165OL@8	10.34		0.88	2.60	0.017	32.2
14YZ-165OL@9	9.54		0.88	2.37	0.015	30.2
14YZ-165OL@10	10.17		0.95	2.13	0.015	29.2
14YZ-165OL@11	7.70		0.91	3.02	0.017	26.1
14YZ-165OL@12	7.76		0.89	3.06	0.021	24.1
14YZ-167OL@1	Dunite		9.74	0.88	2.72	0.016
14YZ-167OL@2		7.98	0.88	2.81	0.017	52.3
14YZ-167OL@3		10.50	0.89	2.50	0.015	42.2
14YZ-167OL@4		7.47	0.89	2.65	0.015	36.2
14YZ-167OL@5		7.04	0.86	2.91	0.017	44.3
14YZ-167OL@6		6.04	0.86	3.31	0.019	40.2
14YZ-167OL@7		3.13	0.86	3.55	0.022	80.5
14YZ-167OL@9		3.17	0.88	2.86	0.017	60.3
14YZ-167OL@10		1.58	0.88	2.74	0.017	80.5
14YZ-167OL@11		1.33	0.89	2.49	0.015	124.7
14YZ-167OL@13		2.67	0.94	3.02	0.018	140.8
14YZ-167OL@16		5.28	0.89	2.84	0.017	60.3

Table 1. Li content, $\delta^7\text{Li}$ values of olivines from the Yunzhug ophiolitic harzburgite and dunite, central Tibet.

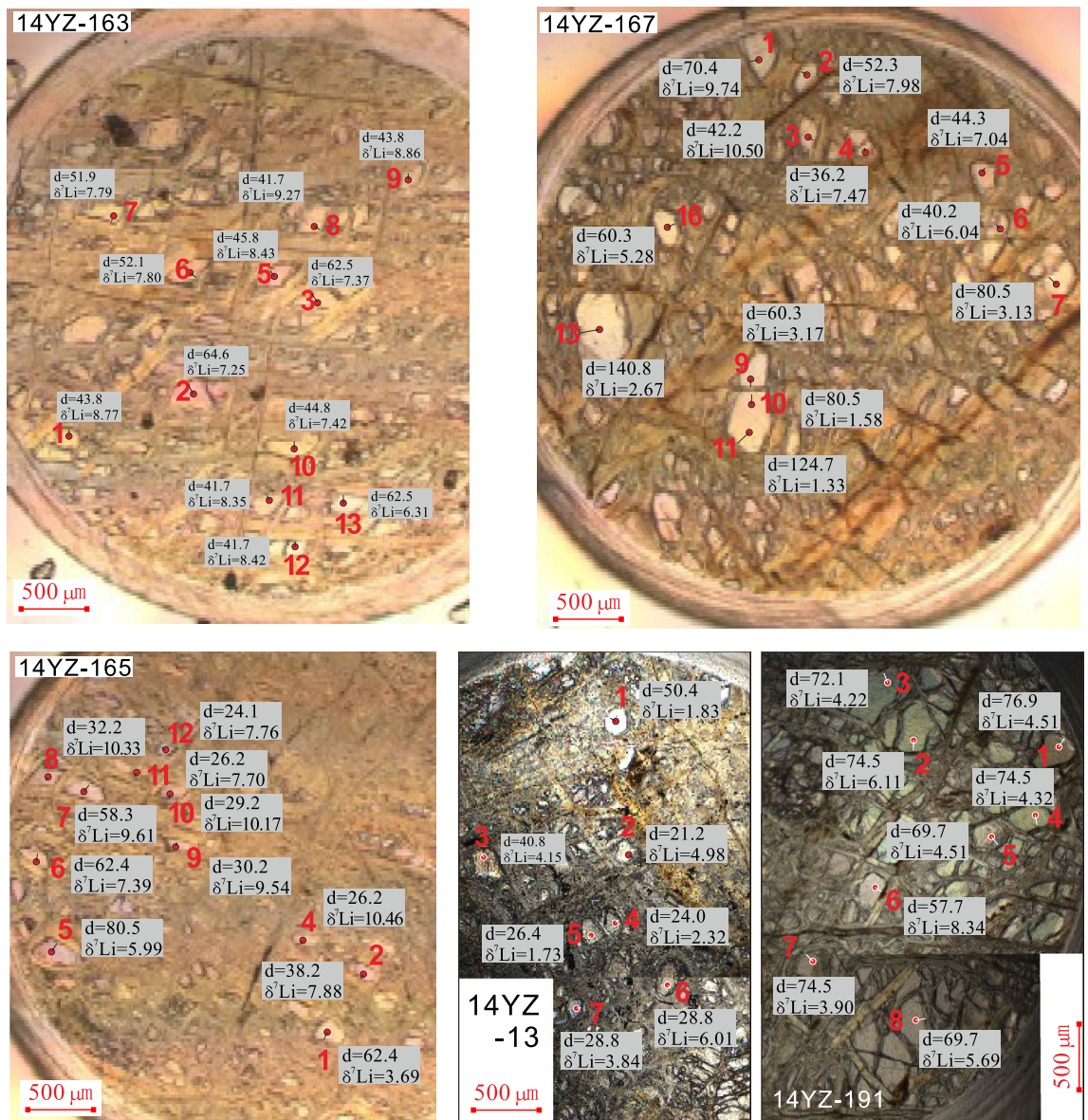


Figure 2. Scanned image of mounts showing olivine grains in the Yunzhug ophiolitic harzburgite and dunite for in situ Li isotope analysis, d = the distance from the rim of each grain.

temperatures. The Li ion surrounding the water with hydration shells likely plays an important role in limiting the isotopic heterogeneity associated with diffusion⁴². Therefore, the seawater Li isotopic characteristics can be preserved in the fresh olivine grains by Li ion diffusion.

Conclusion

The oceanized SCLM peridotites from the Yunzhug ophiolite within the Tibetan Bangong-Nujiang suture zone are characterized by strong Li isotopic disequilibria caused by diffusion of Li from seawater to rocks. Because Li diffuses rapidly at high temperatures during partial melting and melt-rock interactions in the refractory peridotites, Li isotopes should have approached equilibrium before the mantle peridotites were exposed to the seafloor by the detachment during the first stage of Wilson cycle. When the mantle peridotites emerged on the seafloor at lower temperature, Li diffused from seawater to olivine since the Li is a fluid-mobile element and its activity in seawater is significantly higher than that of olivine under low temperature. This study highlights that Li isotopic heterogeneity in olivines of the oceanized SCLM peridotites can be produced by the surficial processes, such as diffusion from seawater.

In situ Li concentration and isotopic compositions

In situ Li elemental and isotopic compositions of olivine were analyzed using a Cameca IMS- 1280HR SIMS at IGGCAS, following established methods⁴³. The samples were coated under vacuum with high-purity gold before the SIMS analysis. The primary oxygen ion beam was accelerated at 13 kV, with an intensity of 25 nA.

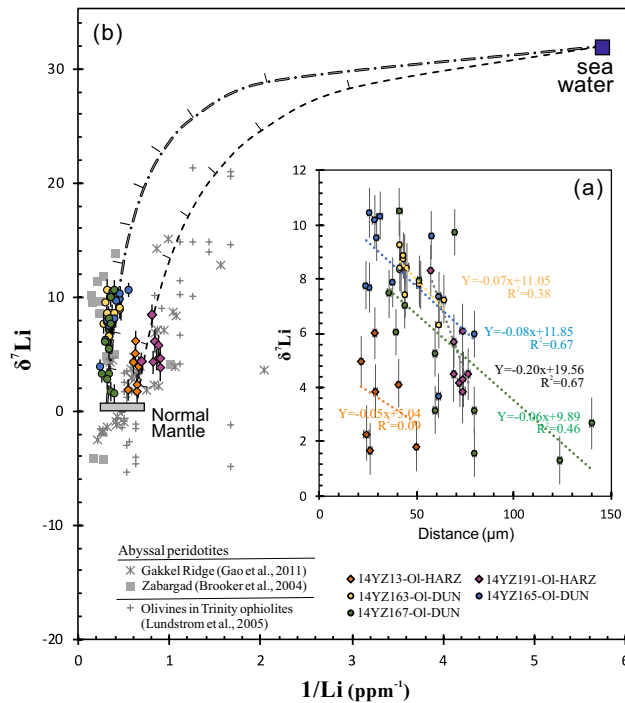


Figure 3. (a) Plot of $\delta^7\text{Li}$ values versus the distance from the rim of olivine grain; (b) $\delta^7\text{Li}$ values and Li content of olivine plot along the mixing line between seawater and subcontinental lithospheric mantle (close to the normal mantle).

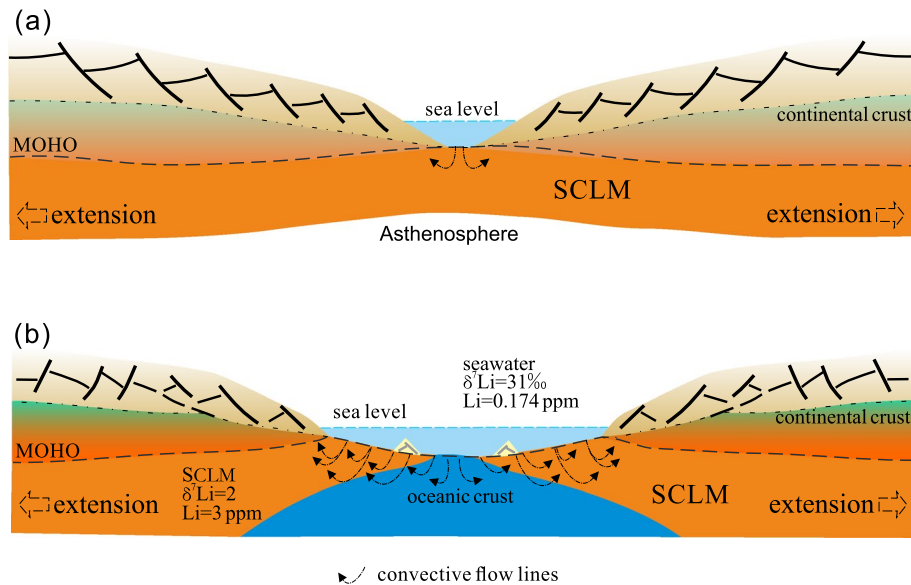


Figure 4. Schematic model showing the processes of seawater Li diffusion into the subcontinental lithospheric mantle (SCLM), (a) seawater initiates contact with SCLM at the rifting of continent associated with the upwelling of asthenosphere by detachment at the early stage of the Wilson cycle; (b) hydrothermal convection of sea-water through still hot, newly-formed oceanic crust cause further diffusion of seawater Li into the SCLM.

The elliptical spot was approximately $20 \times 30 \mu\text{m}$ in size. Positive secondary ions were measured on an electron multiplier in pulse counting mode, with a mass resolution (M/DM) of 1500 and an energy slit open at 40 eV without any energy offset. Eighty cycles were measured with counting times of 7 and 2 s for ^6Li and ^7Li , respectively. The measured $\delta^7\text{Li}$ values are given as $\delta^7\text{Li} \left(\left[\frac{(^7\text{Li}/^6\text{Li})_{\text{sample}}}{(^7\text{Li}/^6\text{Li})_{\text{L-SVEC}}} - 1 \right] \times 1000 \right)$ relative to units of the standard NIST SRM 8545 (L-SVEC) with $^7\text{Li}/^6\text{Li} = 12.0192$. The instrumental mass fractionation (IMF) is

expressed in $\delta^7\text{Li}$ units: $\Delta i = \delta^7\text{Li}_{\text{SIMS}} - \delta^7\text{Li}_{\text{MC-ICPMS}}$. In-house standards used here include two olivines (06JY31: Mg#_90.3; 06JY34: Mg#_91.5), which were detailed described by Su et al. (2015a)⁴³. The olivine 06JY34 is used for those samples with higher Mg# in olivines (sample 14YZ-13; 14YZ-163; 14YZ-165; 14YZ-167; 14YZ-191). The olivine standards in this study yielded an average $\delta^7\text{Li}$ of $4.51 \pm 0.78\text{‰}$ (06JY31_olivine: $n = 10$; 1se), $3.33 \pm 0.72\text{‰}$ (06JY34_olivine: $n = 10$; 1se), consistent with the recommended values⁴⁰. Lithium concentrations of the samples were calculated based on $^7\text{Li}^+$ count rates (cps/nA) relative to the standard⁴³. The detection limit of Li concentration measurements is < 1 ppb and the analytical uncertainties of the Li isotopic compositions are less than 1.5‰ (1se). Previous studies have suggested a substantial matrix effect on the $^7\text{Li}/^6\text{Li}$ ratio of olivine measured by SIMS⁴⁴, with $\delta^7\text{Li}$ increasing by about 1.0‰ for each mole percent decrease in forsterite component⁴³. Thus the measured $\delta^7\text{Li}$ in olivines from studied samples were further corrected as suggested.

Data availability

Data are available through Mendeley Data at <https://data.mendeley.com/datasets/zbfk4p559z/1>.

Received: 28 May 2023; Accepted: 14 February 2024

Published online: 19 February 2024

References

- Batiza, R. Inverse relationship between Sr isotope diversity and rate of oceanic volcanism has implications for mantle heterogeneity. *Nature* **309**, 440–441 (1984).
- Zindler, A. & Hart, S. R. Chemical geodynamics. *Ann. Rev. Earth. Planet. Sci.* **14**, 493–571 (1986).
- Gibson, S. A. Major element heterogeneity in Archean to Recent mantle plume starting-heads. *Earth Planet. Sci. Lett.* **195**, 59–74 (2002).
- Jennings, E. S., Holland, T. J. B., Shorttle, O., MacLennan, J. & Gibson, S. A. The composition of melts from a heterogeneous mantle and the origin of ferropicrite: Application of a thermodynamic model. *J. Petrol.* **57**(11–12), 2289–2310 (2016).
- Su, B. X., Zhou, M. F. & Robinson, P. T. Extremely large fractionation of Li isotopes in chromitite-bearing mantle sequence. *Sci. Rep.* **6**(22370), 11 (2016).
- Su, B. X. et al. Melt penetration in oceanic lithosphere: Li isotope records from the Pozanti-Karsanti ophiolite in Southern Turkey. *J. Petrol.* **59**(1), 191–205 (2018).
- Wang, J. X., Zhou, H. Y., Salters, V. J. M., Dick, H. J. B. & Wang, C. H. Trace element and isotopic evidence for recycled lithosphere at basalts from 48°E to 53°E, Southwest Indian Ridge. *J. Petrol.* <https://doi.org/10.1093/petrology/egaa068> (2020).
- Faure, G. & Mensing, T. M. *Isotopes: Principles and Applications* 3rd edn. (Wiley, 2005).
- Dorland, S. P., Liu, X. M. & Rudnick, R. L. Lithium isotope geochemistry. *Rev. Mineral. Geochem.* **82**(1), 165–217. <https://doi.org/10.2138/rmg.2017.82.6> (2017).
- Strandmann, P. A. E. P., Kasemann, S. A. & Wimpenny, J. B. Lithium and Lithium isotopes in Earth's surface cycles. *Elements* **16**, 253–258 (2020).
- Millot, R., Guerrot, C. & Vigier, N. Accurate and high-precision measurement of lithium isotopes in two reference materials by MC-ICP-MS. *Geostandards Geoanal. Res.* **28**(1), 153–159 (2004).
- Chan, L. H., Edmond, J. M., Thompson, G. & Gillis, K. Lithium isotopic composition of submarine basalts: Implications for the lithium cycle in the oceans. *Earth Planet. Sci. Lett.* **108**(1–3), 151–160 (1992).
- Chan, L. H., Leeman, W. P. & You, C. F. Lithium isotopic composition of Central American volcanic arc lavas: Implications for modification of subarc mantle by slab-derived fluids: Correction. *Chem. Geol.* **182**(2–4), 293–300 (2002).
- Chan, L. H., Alt, J. C. & Teagle, D. A. H. Lithium and lithium isotope profiles through the upper oceanic crust: A study of seawater-basalt exchange at ODP Sites 504B and 896A. *Earth Planet. Sci. Lett.* **201**(1), 187–201 (2002).
- Anonymous. Penrose field conference on ophiolites. *Geotimes* **17**, 24–25 (1972).
- Coleman, R. G. Ophiolites: Ancient oceanic lithosphere? *Miner. Rocks* **12**, 1–229 (1977).
- Huang, X. X. et al. Oceanization of the subcontinental lithospheric mantle recorded in the Yunzhug ophiolite, Central Tibetan Plateau. *Lithos* **370–371**, 10562 (2020).
- Girardeau, J. et al. Tectonic environment and geodynamic significance of the Neo-Cimmerian Dongqiao ophiolite, Bangong-Nujiang suture zone, Tibet. *Nature* **307**, 27–31 (1984).
- Wang, X. B., Bao, P. S., Deng, W. M. & Wang, F. G. Tectonic evolution of Himalayan lithosphere-Tibet ophiolite (3). *Geochem. Pet. Min.* **6**, 138–214 (1987) (in Chinese with English abstract).
- Zhang, Q. & Zhou, G. Q. *Ophiolites of China* 82–92 (China Science Publishing House, 2001).
- Shi, R. D., Yang, J. S., Xu, Z. Q. & Qi, X. X. The Bangong Lake ophiolite (NW Tibet) and its bearing on the tectonic evolution of the Bangong-Nujiang suture zone. *J. Asian Earth Sci.* **32**, 438–457 (2008).
- Moores, E. M. & Vine, F. J. The Troodos Massif, Cyprus and other ophiolites as oceanic crust: Evaluation and implications. *Philos. Trans. R. Soc. B Biol. Sci.* **268**, 443–467 (1971).
- Nicolas, A. & Boudier, F. Mapping oceanic ridge segments in Oman ophiolite. *J. Geophys. Res. Solid Earth* **100**, 6179–6197 (1995).
- Piccardo, G. B., Padovano, M. & Guarnieri, L. The Ligurian Tethys: Mantle processes and geodynamics. *Earth Sci. Rev.* **138**, 409–434 (2014).
- Tomascak, P. B., Langmuir, C. H., le Roux, P. J. & Shirey, S. B. Lithium isotopes in global mid-ocean ridge basalts. *Geochim. Cosmochim. Acta* **72**, 1626–1637 (2008).
- Seitz, H. M., Brey, G. P., Lahaye, Y., Durali, S. & Weyer, S. Lithium isotopic signatures of peridotite xenoliths and isotopic fractionation at high temperature between olivine and pyroxenes. *Chem. Geol.* **212**, 163–177 (2004).
- Bodinier, J. L. & Godard, M. Orogenic ophiolitic, and abyssal peridotites. In *Treatise on Geochemistry* Vol. 2 (ed. Carlson, R. W.) 103–170 (Elsevier, 2003).
- Niu, Y. Bulk-rock major and trace element compositions of abyssal peridotites: Implications for mantle melting melt extraction and post melting processes beneath mid-ocean ridges. *J. Pet.* **45**, 1–36 (2004).
- Le Roux, V. et al. The Iherz spinel Iherzolite: Refertilized rather than pristine mantle. *Earth Planet. Sci. Lett.* **259**, 599–612 (2007).
- Deschamps, F., Godard, M., Guillot, S. & Hattori, K. Geochemistry of subduction zone serpentinites: A review. *Lithos* **178**, 96–127 (2013).
- Rudnick, R. L. & Ionov, D. A. Lithium elemental and isotopic disequilibrium in minerals from peridotite xenoliths from far-east Russia: Product of recent melt/fluid-rock reaction. *Earth Planet. Sci. Lett.* **256**, 278–293 (2007).
- Nishio, Y. et al. Lithium isotopic systematics of the mantle derived ultramafic xenoliths: Implications for EM1 origin. *Earth Planet. Sci. Lett.* **217**, 245–261 (2004).
- Magna, T., Wiechert, U. & Halliday, A. N. New constraints on the lithium isotope compositions of the Moon and terrestrial planets. *Earth Planet. Sci. Lett.* **243**, 336–353 (2006).

34. Jeffcoate, A. B. *et al.* Li isotope fractionation in peridotites and mafic melts. *Geochim. Cosmochim. Acta* **71**, 202–218 (2007).
35. Brooker, R. A., James, R. H. & Blund, J. D. Trace elements and Li isotope systematics in Zabargad peridotites: Evidence of ancient subduction processes in the Red Sea mantle. *Chem. Geol.* **212**, 179–204 (2004).
36. Gao, Y. J. *et al.* Cooling-induced fractionation of mantle Li isotopes from the ultraslow-spreading Gakkel Ridge. *Earth Planet. Sci. Lett.* **301**, 231–240 (2011).
37. Lundstrom, C. C., Chaussidon, M., Hsui, A. T., Kelemen, P. & Zimmerman, M. Observations of Li isotopic variations in the Trinity Ophiolite: Evidence for isotopic fractionation by diffusion during mantle melting. *Geochimica et Cosmochimica Acta* **69**(3), 735–751 (2005).
38. Quick, J. E. Petrology and Petrogenesis of the Trinity Peridotite, an Upper Mantle Diapir in the Eastern Klamath Mountains, Northern California. *J. Geophys. Res.* **86**, 11837–11863 (1981).
39. Elder, J. W. Model of hydrothermal ore genesis. *Geol. Soc. Lond. Spec. Publ.* **7**, 4–13 (1977).
40. Stern, C., de Wit, M. J. & Lawrence, V. R. Igneous and metamorphic processes associated with the formation of Chilean ophiolites and their implication for ocean-floor metamorphism, seismic layering and magnetism. *J. Geophys. Res.* **81**, 4370–4380 (1976).
41. Sheppard, S. M. F. Identification of the origin of ore-forming solutions by the use of stable isotopes. *Geol. Soc. Lond. Spec. Publ.* **7**, 25–41 (1977).
42. Richter, F. M. *et al.* Kinetic isotopic fractionation during diffusion of ionic species in water. *Geochimica et Cosmochimica Acta* **70**, 277–289 (2006).
43. Su, B. X. *et al.* Potential orthopyroxene, clinopyroxene and olivine reference materials for in situ lithium isotope determination. *Geostandards Geoanal. Res.* <https://doi.org/10.1111/j.1751-908X.2014.00313.x> (2015).
44. Bell, D. R., Hervig, R. L., Buseck, P. R. & Aullbach, S. Lithium isotope analysis of olivine by SIMS: Calibration of a matrix effect and application to magmatic phenocrysts. *Chem. Geol.* **258**, 5–16 (2009).

Acknowledgements

This study was supported by the Second Tibetan Plateau Scientific Expedition and Research Program (STEP), Grant No. 2019QZKK0703, and the National Natural Science Foundation of China (Grants 92062215, 41972052).

Author contributions

R.-D.S., Q.-S.H., and X.-X.H. collected the samples. Q.-S.H., X.-X.H., G.-H.C., and X.-H.G. conducted the chemical analyses. R.-D.S. and H.-B.Z. wrote the main manuscript text. G.-H.C. prepared the Figs. 1, 2 and 3 and table. J.-S.Y. made important suggestions for the genesis of OCT ophiolitic peridotites. All authors contributed equally to the intellectual growth of this paper.

Competing interests

The authors declare no competing interests.

Additional information

Correspondence and requests for materials should be addressed to R.-D.S.

Reprints and permissions information is available at www.nature.com/reprints.

Publisher's note Springer Nature remains neutral with regard to jurisdictional claims in published maps and institutional affiliations.



Open Access This article is licensed under a Creative Commons Attribution 4.0 International License, which permits use, sharing, adaptation, distribution and reproduction in any medium or format, as long as you give appropriate credit to the original author(s) and the source, provide a link to the Creative Commons licence, and indicate if changes were made. The images or other third party material in this article are included in the article's Creative Commons licence, unless indicated otherwise in a credit line to the material. If material is not included in the article's Creative Commons licence and your intended use is not permitted by statutory regulation or exceeds the permitted use, you will need to obtain permission directly from the copyright holder. To view a copy of this licence, visit <http://creativecommons.org/licenses/by/4.0/>.

© The Author(s) 2024